

Ruthenium(II) Complexes with Chiral Tetradentate P₂N₂ Ligands Catalyze the Asymmetric Epoxidation of Olefins with H₂O₂

Robert M. Stoop, Stephan Bachmann, Massimiliano Valentini,[†] and Antonio Mezzetti*

Laboratory of Inorganic Chemistry, Swiss Federal Institute of Technology, ETH Zentrum, CH-8092 Zürich, Switzerland

Received June 7, 2000

The five-coordinate complexes of the type [RuCl(PNNP)]PF₆ (PNNP = tetradentate ligand with a P₂N₂ donor set) are prepared by chloride abstraction from [RuCl₂(PNNP)]. A mixture of Δ -*cis*- β - and Λ -*cis*- β -[RuCl₂(**1a**- κ^4 P,N,N,P)] (**2a**; **1a** = *N,N*-bis[*o*-(diphenylphosphino)benzylidene]-2,2'-diimino-1,1'-(*S*)-binaphthylene), prepared by reaction of **1a** with [RuCl₂(PPh₃)₃], reacts with Ti[PF₆], giving the five-coordinate [RuCl(**1a**- κ^4 P,N,N,P)]PF₆ (**3a**). The related *trans*-[RuCl₂(**1b**- κ^4 P,N,N,P)] (**2b**; **1b** = *N,N*-bis[*o*-(diphenylphosphino)benzylidene]-(1*S*,2*S*)-diiminocyclohexane) reacts with Ti[PF₆] to give [RuCl(**1b**- κ^4 P,N,N,P)]PF₆ (**3b**). With the amino ligand *N,N*-bis[*o*-(diphenylphosphino)benzylidene]-(1*S*,2*S*)-diaminocyclohexane (**1c**), the aqua complex [RuCl(OH₂)(**1c**- κ^4 P,N,N,P)]PF₆ (**5c**) is obtained by reaction of Ti[PF₆] with [RuCl₂(PPh₃)(**1c**- κ^3 P,N,N)] (**4**), which has been isolated and structurally characterized. The reactivity of the five-coordinate **2b** with CO and oxygen donors such as water, Et₂O, THF, and methanol is reported. Both **3** and **5** catalyze the asymmetric epoxidation of olefins with hydrogen peroxide as oxidant. Enantiomeric excesses up to 42% were obtained in the enantioselective epoxidation of styrene and of other unfunctionalized olefins. The reaction is highly stereospecific, as the epoxidation of (*Z*)-2-methylstyrene gives a *cis:trans* ratio of 99:1.

Introduction

The enantioselective catalytic epoxidation of olefins is an essential synthetic method.¹ Despite the fact that recent breakthroughs have been achieved in this field, several problems are still unresolved. These concern, in particular, the nature of the oxidant and the product selectivity. Thus, Mn–salen catalysts give excellent enantioselectivity for tri- and *cis*-disubstituted olefins, but partial loss of configuration occurs.¹ Also, the enantioselectivity with mono- or *trans*-disubstituted olefins is much lower.¹ As for the oxidant, the best results are obtained with expensive or environmentally nonbenign oxidants, such as iodosyl benzene and hypochlorite. Clearly, the ideal oxidant is molecular oxygen or, even better, air, but this goal remains far away.²

After dioxygen, hydrogen peroxide is considered the most environmentally friendly and economic of oxidants,³ but a number of problems hamper its use in (asymmetric) oxidation reactions. In addition to the

intrinsic danger related with concentrated H₂O₂ solutions, there is the decomposition reaction catalyzed by most transition metals and the handling of a biphasic system.³ Also, water generally deactivates most oxidation catalysts due to strong coordination to the metal center. Finally, much lower enantioselectivities are generally obtained with hydrogen peroxide than with hypochlorite or PhIO.^{4–7} Thus, there is considerable interest in developing enantioselective catalytic systems as an alternative to the manganese-based ones.

Ruthenium complexes containing nitrogen-donor ligands have been largely investigated in asymmetric oxidation catalysis. Thus, ruthenium complexes containing porphyrin,⁸ oxazoline,⁹ or salen¹⁰ chiral ligands

* To whom correspondence should be addressed. E-mail: mezzetti@inorg.chem.ethz.ch.

[†] Spin-diffusion measurements.

(1) For recent reviews, see: (a) Ito, Y. N.; Katsuki, T. *Bull. Chem. Soc. Jpn.* **1999**, *72*, 603. (b) Jacobsen, E. N. In *Catalytic Asymmetric Synthesis*; Ojima, I., Ed.; VCH: New York, 1993; Chapter 4.2.

(2) (a) *The Activation of Dioxygen and Homogeneous Catalytic Oxidation*; Barton, D. H. R., Martell, A. E., Sawyer, D. T., Eds.; Plenum: New York, 1993. (b) James, B. R. *Dioxygen Activation and Homogeneous Catalytic Oxidation*; Simandi, L. I., Ed.; Elsevier: Amsterdam, 1991; p 195. Selected examples: (c) Groves, J. T.; Quinn, R. J. *Am. Chem. Soc.* **1985**, *107*, 5790. (d) Neumann, R.; Dahan, M. *Nature* **1997**, *388*, 353. (e) Neumann, R.; Dahan, M. *J. Am. Chem. Soc.* **1998**, *120*, 11969.

(3) Strukul, G., Ed. *Catalytic Oxidation with Hydrogen Peroxide as Oxidant*; Kluwer: Dordrecht, The Netherlands, 1992.

(4) See, for instance: Katsuki, T. *J. Mol. Catal. A: Chem.* **1996**, *113*, 87.

(5) (a) Berkessel, A.; Frauenkron, M.; Schwenkreis, T.; Steinmetz, A. *J. Mol. Catal. A: Chem.* **1997**, *117*, 339. (b) Berkessel, A.; Frauenkron, M.; Schwenkreis, T.; Steinmetz, A.; Baum, G.; Fenske, D. *J. Mol. Catal. A: Chem.* **1996**, *113*, 321. (c) Schwenkreis, T.; Berkessel, A. *Tetrahedron Lett.* **1993**, *34*, 4785.

(6) Bolm, C.; Kadereit, D.; Valacchi, M. *Synlett* **1997**, 687.

(7) (a) Pietikäinen, P. *Tetrahedron* **1998**, *54*, 4319. (b) Pietikäinen, P. *Tetrahedron Lett.* **1994**, *35*, 941.

(8) (a) Groves, J. T.; Viski, P. *J. Org. Chem.* **1990**, *55*, 3628 and references therein. (b) O'Malley, S.; Kodadek, T. *J. Am. Chem. Soc.* **1989**, *111*, 9116. (c) Mansuy, D.; Battioni, P.; Renaud, J. P.; Guerin, P. *J. Chem. Soc., Chem. Commun.* **1985**, 155. (d) Zhang, R.; Yu, W. Y.; Lai, T. S.; Che, C. M. *Chem. Commun.* **1999**, 409. (e) Gross, Z.; Ini, S. *J. Org. Chem.* **1997**, *62*, 5514. (f) Berkessel, A.; Frauenkron, M. *J. Chem. Soc., Perkin Trans. 1* **1997**, 2265.

(9) (a) End, N.; Pfaltz, A. *Chem. Commun.* **1998**, 589. (b) Nishiyama, H.; Shimada, T.; Itoh, H.; Sugiyama, H.; Motoyama, Y. *Chem. Commun.* **1997**, 1863.

Scheme 1

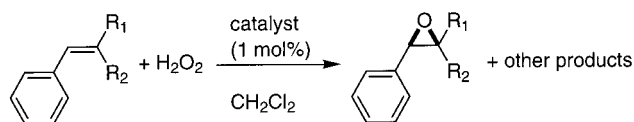
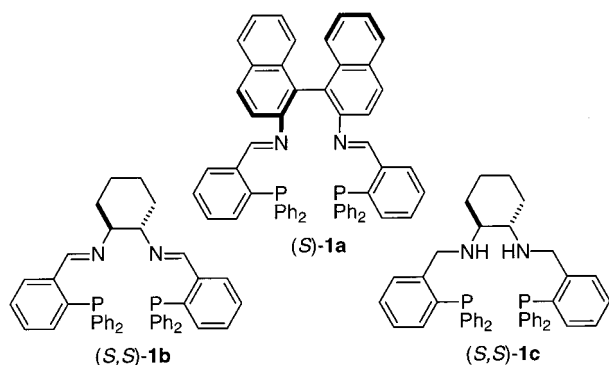


Chart 1



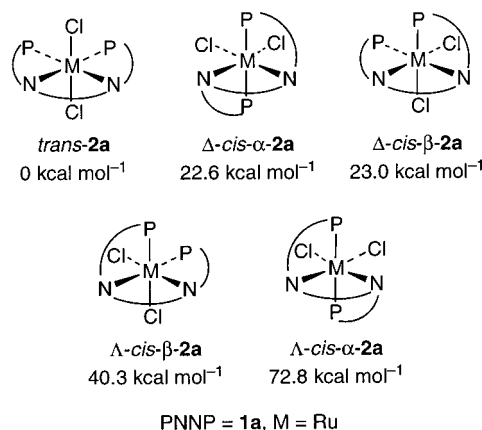
have been successfully used in asymmetric epoxidation of unfunctionalized olefins, in particular *trans*-disubstituted ones. However, the use of H_2O_2 as oxidant together with ruthenium catalysts is particularly rare^{11–13} and is unprecedented in asymmetric catalysis, whereas phosphine complexes of platinum have been successfully used in asymmetric (ep)oxidation reactions with H_2O_2 as the oxidant.¹⁴

Thus, following early reports of the use of phosphine complexes in catalytic oxidation,¹⁵ we investigated the use of five-coordinate chiral complexes of the type $[\text{RuCl}(\text{P}-\text{P}^*)]^+$ as epoxidation catalysts ($\text{P}-\text{P}^* =$ chiral diphosphine).¹⁶ Recently, we have also found that the cationic complexes $[\text{RuCl}(\text{PNPP})]\text{PF}_6$ (where PNPP is a tetradentate chiral ligand containing two imines and two phosphines) catalyze the asymmetric epoxidation of unfunctionalized olefins with hydrogen peroxide as the primary oxidant (Scheme 1).¹⁷ We report here in full on the ruthenium coordination chemistry of the PNPP ligands depicted in Chart 1, as well as on their application in the enantioselective epoxidation of a number of unfunctionalized olefins with aqueous hydrogen peroxide as the oxidant.

Results and Discussion

Synthesis of the PNPP Ligands. The ligands *N,N*-bis[*o*-(diphenylphosphino)benzylidene]-2,2'-diimino-1,1'-

Chart 2



PNPP = **1a**, M = Ru

(*S*)-binaphthylene (**1a**) and *N,N*-bis[*o*-(diphenylphosphino)benzylidene]-(1*S*,2*S*)-diiminocyclohexane (**1b**) are best prepared by condensation of $\text{Ph}_2\text{P}(o\text{-CHO-C}_6\text{H}_4)$ (2 equiv) with the corresponding enantiomerically pure diamine. This procedure avoids the racemate resolution process that has been previously reported for **1b**.¹⁸ The amino analogue **1c** was prepared according to the reported procedure, which involves NaBH_4 reduction of **1b** in ethanol solution.¹⁸ All ligands are crystalline solids and are stable with respect to oxidation and hydrolysis. The ligands **1b,c** have been used in the asymmetric ruthenium-catalyzed transfer hydrogenation of ketones,¹⁹ whereas the ligand (*S*)-**1a** is new.²⁰

[RuCl(1a**-κ⁴P,N,N,P)]PF₆.** The reaction of $[\text{RuCl}_2(\text{PPh}_3)_3]$ with the binaphthyl ligand **1a** in boiling benzene or toluene gives *trans*- $[\text{RuCl}_2(\mathbf{1a}\text{-}\kappa^4\text{P,N,N,P})]$ (*trans*-**2a**) as the only product, as indicated by the singlet at δ 46.3 in the ³¹P NMR spectrum. However, *trans*-**2a** failed to react with $\text{Ti}[\text{PF}_6]$ in CH_2Cl_2 , CHCl_3 , or boiling benzene. Thus, we prepared **2a** as a mixture of the *trans* and *cis* isomers by reacting $[\text{RuCl}_2(\text{PPh}_3)_3]$ and **1a** in CH_2Cl_2 at room temperature. This procedure affords **2a** as a mixture of the Δ-*cis*-β, Λ-*cis*-β, and *trans* isomers in a 5:4:1 ratio, as determined by ³¹P NMR spectroscopy. The minor *cis* isomer *cis*-β-**2a''** (40%), which exhibits two doublets at δ 49.4 and 41.4 ($J_{\text{PP}'} = 31.9$ Hz) was separated from the other two isomers *cis*-β-**2a'** (50%, two doublets at δ 52.1 and 43.3, $J_{\text{PP}'} = 33.5$ Hz) and *trans*-**2a** (10%) by column chromatography.

To attribute, at least tentatively, the absolute configuration at the metal in **2a–c**, we calculated the relative energies of the diastereomeric complexes $[\text{RuCl}_2(\text{PNPP})]$ by means of molecular modeling (Cerius²)²¹ (Charts 2–4). For all three ligands **1a–c**, the *trans* isomer is the least strained one and should be the thermodynamic product as far as steric factors are

(10) (a) Takeda, T.; Irie, R.; Shinoda, Y.; Katsuki, T. *Synlett* **1999**, 1157. (b) Kureshi, R. I.; Khan, N. H.; Abdi, S. H. R.; Iyer, P. *J. Mol. Catal. A: Chem.* **1997**, 124, 91.

(11) Sheldon, R. A.; Barf, G. A. *J. Mol. Catal. A: Chem.* **1995**, 102, 23.

(12) Fisher, J. M.; Fulford, A.; Bennett, P. S. *J. Mol. Catal.* **1992**, 77, 229.

(13) Behr, A.; Eusterwiemann, K. *J. Organomet. Chem.* **1991**, 403, 215.

(14) (a) Baccin, C.; Gusso, A.; Pinna, F.; Strukul, G. *Organometallics* **1995**, 14, 1161. (b) Gusso, A.; Baccin, C.; Pinna, F.; Strukul, G. *Organometallics* **1994**, 13, 3442. (c) Sinigaglia, R.; Michelin, R. A.; Pinna, F.; Strukul, G. *Organometallics* **1987**, 6, 728.

(15) (a) Bressan, M.; Morvillo, A. *Inorg. Chem.* **1989**, 28, 950. (b) Morvillo, A.; Bressan, M. *J. Mol. Catal. A: Chem.* **1997**, 125, 119. (c) Maran, F.; Morvillo, A.; d'Alessandro, N.; Bressan, M. *Inorg. Chim. Acta* **1999**, 288, 122.

(16) Stoop, R. M.; Bauer, C.; Setz, P.; Wörle, M.; Wong, T. Y. H.; Mezzetti, A. *Organometallics* **1999**, 18, 5691.

(17) Stoop, R. M.; Mezzetti, A. *Green Chem.* **1999**, 39.

(18) Wong, W. K.; Chik, T. W.; Hui, K. N.; Williams, I.; Feng, X.; Mak, T. C. W.; Che, C. M. *Polyhedron* **1996**, 15, 4447.

(19) Gao, J. X.; Ikariya, T.; Noyori, R. *Organometallics* **1996**, 15, 1087.

(20) The synthesis of the racemic ligand **1a** has been previously reported: (a) Wong, W. K.; Gao, J. X.; Wong, W. T.; Che, C. M. *Polyhedron* **1993**, 12, 2063. (b) Wong, W. K.; Gao, J. X.; Wong, W. T.; Cheng, W. C.; Che, C. M. *J. Organomet. Chem.* **1994**, 277.

(21) Cerius² is a molecular modeling program based on the universal force field (UFF): Rappé, A. K.; Casewit, C. J.; Colwell, K. S.; Goddard, W. A., III; Skiff, W. M. *J. Am. Chem. Soc.* **1992**, 114, 10024. Rappé, A. K.; Colwell, K. S.; Casewit, C. J. *Inorg. Chem.* **1993**, 32, 3438. PDB files of the minimized structures are available from the authors on request.

Chart 3

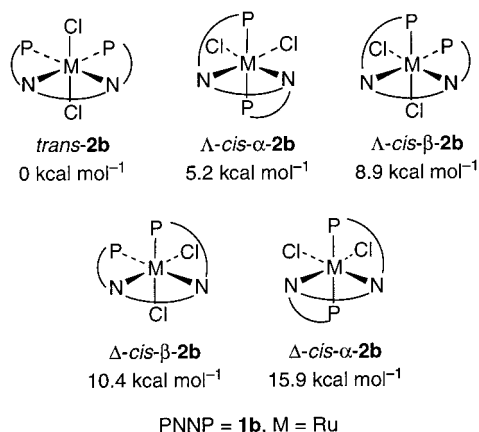
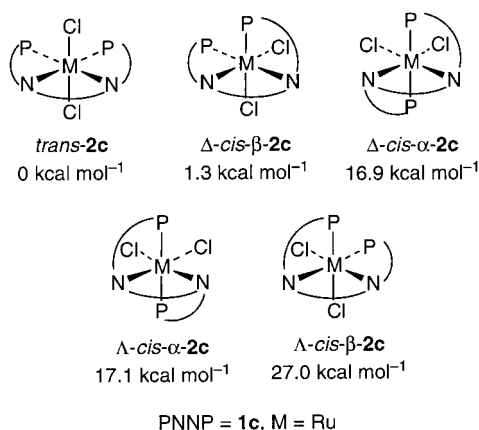


Chart 4



concerned. However, a perusal of the energy data reveals that electronic factors, which are not taken into account in the UFF calculation, clearly influence the relative stability of the isomers. Thus, Cerius² calculations suggest that one *cis*-α isomer of **2a,b** is more stable than both *cis*-β isomers, but no *cis*-α isomer has ever been observed. Indeed, a *trans* arrangement of the phosphines is disfavored due to the competition for the same π -electrons of ruthenium. Assuming that the equilibrium composition (i.e., 100% *trans* isomer) is reached through intermediates of descending energy, then the last *cis*-β isomer observed (either Δ or Λ) should be the most stable one. However, in the case of **2a**, the nearly equal distribution of the *cis*-β isomer **2a'** (50%) and **2a''** (40%) precludes even a tentative attribution of the absolute (Δ or Λ) configuration at the metal.

The mixture of the three isomers of **2a** was used as such in the reaction with $\text{Ti}[\text{PF}_6]_3$ to yield the red-brown five-coordinate $[\text{RuCl}(\mathbf{1a}-\kappa^4\text{P,N,N,P})]^+$ (**3a**) as a single isomer. The insoluble *trans* isomer does not react and is filtered off upon crystallization. The isomer mixture consisting of *cis*-β-**2a''** and *trans*-**2a** (3:1, obtained by column chromatography) was treated with $\text{Ti}[\text{PF}_6]_3$ in an NMR tube (CDCl_3). Monitoring of the reaction by means of ^{31}P NMR spectroscopy showed that the (major) isomer *cis*-β-**2a'** is converted into the (minor) one *cis*-β-**2a''**, which reacts in turn to give $[\text{RuCl}(\mathbf{1a}-\kappa^4\text{P,N,N,P})]^+$ (**3a**), whereas *trans*-**2a** remains unchanged. The stable five-coordinate species $[\text{RuCl}(\mathbf{1a}-\kappa^4\text{P,N,N,P})]^+\text{PF}_6^-$ (**3a**) was characterized by elemental analysis, FAB⁺ MS, and ^{31}P and ^1H NMR spectroscopy. The ^{31}P NMR

spectrum of **3a** shows an AX system with δ 79.8 and 44.5 and a $J_{\text{P,P'}}$ coupling constant of 27.6 Hz, indicating mutually *cis* P atoms. The high-frequency resonance at δ 79.8 is diagnostic of five-coordinate Ru(II) complexes containing a five-membered P–Ru–N chelate ring.^{22,23} Addition of 1 equiv of NET_4Cl to **3a** in CDCl_3 quantitatively yields the minor *cis*-β isomer **2a''** as expected on the basis of microscopic reversibility.

[RuCl(1b**- $\kappa^4\text{P,N,N,P}$)]PF₆.** The ligand **1b** reacts with $[\text{RuCl}_2(\text{PPh}_3)_3]$ in CH_2Cl_2 at room temperature, giving the corresponding six-coordinate dichloro complex $[\text{RuCl}_2(\mathbf{1b}-\kappa^4\text{P,N,N,P})]$ (**2b**). Under these conditions, **2b** is obtained as a 1:4 mixture of the *cis*-β and the *trans* isomer, respectively (Chart 3). The isomer distribution is based on the ^{31}P NMR spectrum, where the singlet at δ 47.7 is attributed to the *trans* isomer, as supported by the X-ray structure of *trans*-**2b**.¹⁹ The latter has been obtained by Noyori as the major product of the reaction of **1b** and $[\text{RuCl}_2(\text{dmsO})_4]$ in boiling toluene.¹⁹ We tentatively attribute the configuration at ruthenium in the *cis*-β isomer as Λ -*cis*-β on the basis of molecular modeling, which indicates that the Λ -*cis*-β isomer is 1.5 kcal mol⁻¹ more stable than the Δ -*cis*-β one (Chart 3), but caution is required in view of the very small energy difference.

In contrast with **2a**, both *trans*-**2b** and *cis*-β-**2b** react with $\text{Ti}[\text{PF}_6]_3$ in dry CH_2Cl_2 , giving the red-brown monochloro complex $[\text{RuCl}(\mathbf{1b}-\kappa^4\text{P,N,N,P})]\text{PF}_6^-$ (**3b**), as indicated by the ^{31}P NMR spectra of the reaction between **2b** (4:1 *trans/cis* mixture) and $\text{Ti}[\text{PF}_6]_3$. Thus, the isomeric mixture of **2b** was used in the preparation of **3b** as such. Complex **3b** tenaciously retains variable amounts of the solvents used for crystallization, including hexane, which results in inaccurate elemental analyses. However, its formulation is supported by mass spectrometry (FAB⁺), showing an $[\text{M} + 1]^+$ peak at m/z 796. The cationic nature of **3b** is confirmed by its molar conductivity ($\Lambda_{\text{M}} = 40 \Omega^{-1} \text{cm}^2 \text{mol}^{-1}$ in $10^{-3} \text{mol dm}^{-3}$) in CH_2Cl_2 solution. Together with the unexceptional ^{31}P NMR signal observed for the $[\text{PF}_6]^-$ anion, this rules out the coordination of the anion to ruthenium. Complex **3b** is extremely reactive toward water and other oxygen donors in CH_2Cl_2 or CDCl_3 solution, which restricts the scope of solvents that can be used without forming six-coordinate adducts (see below).

In rigorously dry CD_2Cl_2 or CDCl_3 solutions, the ^{31}P NMR spectrum of **3b** consists of an AX system (δ 49.7 and 59.0) with a $J_{\text{P,P'}}$ coupling constant of 28.2 Hz. The presence of inequivalent, mutually *cis* P atoms is consistent with the bent arrangement of the tetradentate ligand of the *cis*-β isomers in Chart 3. However, the chemical shifts are lower than expected for a five-coordinate complex. In fact, the related five-coordinate complex $[\text{RuCl}(\text{Ph}_2\text{PCH}_2\text{CH}_2\text{NMe}_2)_2]^+$, whose mononuclear nature is supported by a X-ray study, shows a singlet at δ 77.5 in the ^{31}P NMR spectrum.²² Similarly, $[\text{RuCl}(\text{ppye})_2]^+$ (ppye = 1-(diphenylphosphino)-2-(2-pyridyl)ethane) displays a ^{31}P NMR singlet at δ 70.5.²³ Moreover, the latter complex dimerizes in solution and in the solid state, forming the binuclear dication $[(\text{ppye})_2\text{Ru}(\mu\text{-Cl})_2\text{Ru}(\text{ppye})_2]^{2+}$, which has been

(22) Shen, J. Y.; Slugovc, C.; Wiede, P.; Mereiter, K.; Schmid, R.; Kirchner, K. *Inorg. Chim. Acta* **1998**, 268, 69.

(23) Costella, L.; Del Zotto, A.; Mezzetti, A.; Zangrando, E.; Rigo, P. *J. Chem. Soc., Dalton Trans.* **1993**, 3001.

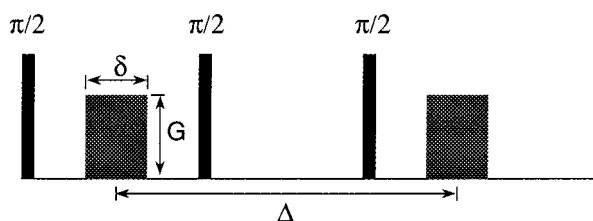


Figure 1. Stimulated echo pulse sequence used for diffusion measurements. δ is the length of the gradient pulse, G its strength, and Δ the time allowed for diffusion.

characterized by X-ray diffraction.²³ Thus, we suspected that **3b** is present, at least in solution, as the doubly chloro-bridged binuclear species $[(\mathbf{1b}-\kappa^4P,N,N,P)Ru(\mu-Cl)_2Ru(\mathbf{1b}-\kappa^4P,N,N,P)]^{2+}$, containing two six-coordinate ruthenium centers. To assess the nuclearity of **3b**, we performed spin-diffusion measurements (see below).

The diffusion coefficients of **3a** and $[RuCl(CO)(\mathbf{1b}-\kappa^4P,N,N,P)]PF_6$ (**6**) were measured by 1H NMR spectroscopy in $CDCl_3$ solution. Complex **6**, which is known to be a mononuclear complex, was chosen as reference. The diffusion coefficient (D) was obtained from pulsed field gradient spin-echo (PGSE) experiments²⁴ with the pulse sequence in Figure 1 systematically changing the strength of the gradient G .²⁵ Plots of the relative intensity of the NMR signals, $\ln(I/I_0)$, vs the square of the gradient amplitude are linear (Figure S1; Supporting Information). Their slopes are directly proportional to the diffusion coefficients D according to eq 1, which

$$\ln\left(\frac{I}{I_0}\right) = -(\gamma\delta)^2 G^2 \left(\Delta - \frac{\delta}{3}\right) D \quad (1)$$

was used to fit the experimental data. As D is correlated to the radii of the molecules,²⁶ and the difference for the slopes is less than 1%, **3a** and **6** have almost the same hydrodynamic radii; i.e., both **6** and **3a** are mononuclear species.

Reaction of $[RuCl_2(PPh_3)_n(\mathbf{1c})]$ ($n = 0, 1$) with $Tl[PF_6]$. As the reaction of $trans-[RuCl_2(\mathbf{1c}-\kappa^4P,N,N,P)]$ (**2c**) with $Tl[PF_6]$ gave no identifiable products, we attempted to prepare *cis*-**2c** as described above. In contrast with **1a,b**, the room-temperature reaction of $[RuCl_2(PPh_3)_3]$ with **1c** in CH_2Cl_2 yielded a mixture of different products rather than of diastereomers. In the typical reaction outcome, the products formed are the reaction intermediate $[RuCl_2(PPh_3)(\mathbf{1c}-\kappa^3P,N,N)]$ (**4**) (60%) (see below), the already reported¹⁹ *trans*-**2c** (10%), and a further species which we tentatively formulate as *cis*- β -**2c** (30%). Accordingly, the FAB⁺ mass spectrum of the product mixture of **2c** and **4** shows the fragmentation pattern expected for $[RuCl_2(\mathbf{1c}-\kappa^4P,N,N,P)]$ along with the molecular peak of **4**. As a further support for the formulation of *cis*- β -**2c**, *trans*-**2c** is obtained quantitatively by refluxing the mixture of *trans*-**2c** and *cis*- β -**2c** (separated by column chromatography from **4**) in

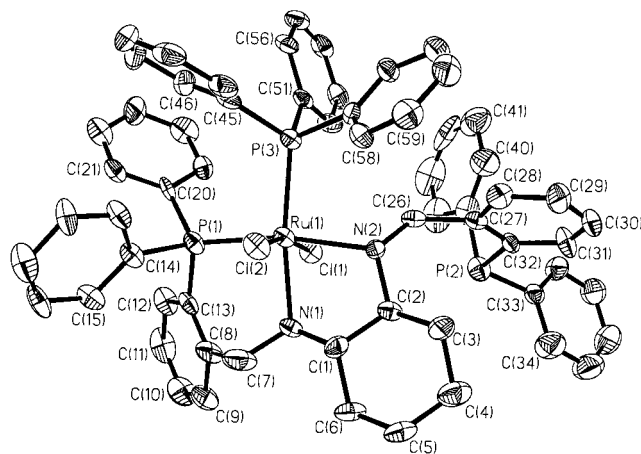


Figure 2. ORTEP view of $[RuCl_2(PPh_3)(\mathbf{1c}-\kappa^3P,N,N)]$ (**4**) (30% probability ellipsoids).

Table 1. Selected Bond Distances (Å) and Angles (deg) for $[RuCl_2(PPh_3)(\mathbf{1c}-\kappa^4P,N,N,P)]$ (**4**)

Ru–N(1)	2.157(9)	Ru–N(2)	2.231(8)
Ru–P(1)	2.280(3)	Ru–P(3)	2.346(3)
Ru–Cl(1)	2.462(3)	Ru–Cl(2)	2.403(3)
N(1)–Ru–N(2)	78.5(3)	N(1)–Ru–P(1)	90.6(3)
N(2)–Ru–P(1)	169.0(2)	N(1)–Ru–P(3)	170.0(3)
N(2)–Ru–P(3)	92.2(2)	P(1)–Ru–P(3)	98.8(1)
N(1)–Ru–Cl(2)	87.0(2)	N(2)–Ru–Cl(2)	88.9(2)
P(1)–Ru–Cl(2)	92.2(1)	P(3)–Ru–Cl(2)	89.2(1)
N(1)–Ru–Cl(1)	79.4(2)	N(2)–Ru–Cl(1)	88.2(2)
P(1)–Ru–Cl(1)	88.3(1)	P(3)–Ru–Cl(1)	104.2(1)
Cl(2)–Ru–Cl(1)	166.4(1)		

C_6D_6 . On the basis of the large energy difference between Δ -*cis*- β -**2c** and Λ -*cis*- β -**2c** (25.7 kcal mol^{−1}), the configuration at ruthenium in *cis*- β -**2c** is most probably Δ (Chart 4).

The PPh_3 adduct $[RuCl_2(PPh_3)(\mathbf{1c}-\kappa^3P,N,N)]$ (**4**) was isolated from the reaction mixture by column chromatography and fully characterized, including an X-ray investigation. The ^{31}P NMR spectrum of **4** shows two doublets for the coordinated P atom of the PNNP ligand and for PPh_3 at δ 46.5 and 38.8. The dangling P atom of the PNNP ligand appears as a singlet at δ −14.7, close to the value of the free ligand (δ −15.9). Single crystals of **4** were obtained by slow diffusion of CH_2Cl_2 into Pr^iOH . The results of the X-ray study are summarized in Figure 2 and Table 1. Along with the complex, the unit cell contains one molecule of CH_2Cl_2 as solvent of crystallization. The complex has a distorted-octahedral coordination with *trans* chlorides and a meridional arrangement of the coordinated P,N,N moiety. The Ru–Cl, Ru–P, and Ru–N distances are in the range expected for similar complexes of general formula $[RuCl_2N_2P_2]$.^{19,22,27} Interestingly, N(1) is more tightly bound to ruthenium than N(2) (2.157(9) vs 2.231(8) Å). This is also reflected by the Ru–P distances, as the PPh_3 ligand is less tightly bound than the PPh_2 group of the PNNP ligand (2.346(3) vs 2.280(3) Å). There are two possible reasons for the relatively long Ru–N(2) and Ru–P(3) distances as compared to Ru–N(1) and Ru–P(1), namely the weaker (or absent) chelate effect or the steric interaction between PPh_3 and the $-o-C_6H_4-PPh_2$ group. Both effects also explain the lability of the PPh_3

(24) Stilbs, P. *Prog. Nucl. Magn. Reson.* **1987**, *19*, 1 and references therein.

(25) Examples of this method: (a) Valentini, M.; Pregosin, P. S.; Rüegger, H. *Organometallics* **2000**, *19*, 2551. (b) Pichota, A.; Pregosin, P. S.; Valentini, M.; Würle, M.; Seebach, D. *Angew. Chem., Int. Ed. Engl.* **2000**, *39*, 153. (c) Jiang, Q.; Rüegger, H.; Venanzi, L. M. *Inorg. Chim. Acta* **1999**, *290*, 64.

(26) This relationship is expressed from the Stokes–Einstein equation: $D = kT/6\pi\eta r_H$, where η is the viscosity of the solution and r_H the hydrodynamic radius.

(27) Song, J. H.; Cho, D. J.; Jeon, S. J.; Kim, Y. H.; Kim, T. J.; Jeong, J. H. *Inorg. Chem.* **1999**, *38*, 893.

ligand. The dangling P atom is 5.58 Å away from ruthenium. The closing of the Cl(1)–Ru–Cl(2) angle (166.4(1)°) reflects the steric crowding and chelate ring strain in the complex, as the chloro ligands are pushed away from the bulky PPh₃ toward the amino moiety *trans* to it. The bite angles for the P,N and N,N chelate rings are 90.6(3) and 78.5(3)°, respectively. The cyclohexyl ring has a regular chair conformation.

[RuCl(L)(PNNP)]PF₆. We investigated the reactivity of the 16-electron complex **3b** toward small molecules such as CO, H₂O, and other N- or O-donors (L) to give the octahedral adducts [RuCl(L)(PNNP)]PF₆ (see Experimental Section).

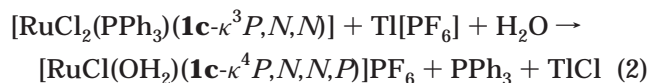
The cationic species [RuCl(**1b**-κ⁴P,N,N,P)]⁺ (**2b**) reacts instantaneously with CO in CH₂Cl₂ at room temperature, giving [RuCl(CO)(**1b**-κ⁴P,N,N,P)]PF₆ (**6**). In this product, the CO ligand occupies the position *trans* to a phosphine, as indicated by the ³¹P and ¹³C NMR data (*J*_{P,C} = 110.0 Hz, *J*_{P,C} = 15.1 Hz). The ν(CO) stretching vibration of **6** (2016 cm⁻¹, KBr) is slightly higher than in similar cationic complexes featuring a *trans* P–Ru–CO moiety, such as [RuCl(CO)(ppy-P,N)₂]⁺ (1996 cm⁻¹)²³ and [RuCl(CO)(Ph₂PCH₂CH₂NMe₂)₂]⁺ (1989 cm⁻¹).²² The comparison between **6** and the latter species suggests that the [RuCl(**1b**-κ⁴P,N,N,P)]⁺ fragment is more electron poor than [RuCl(Ph₂PCH₂CH₂NMe₂)₂]⁺ and, thus, a stronger Lewis acid, as expected from the ligand **1** being a weaker donor than Ph₂PCH₂CH₂NMe. Upon refluxing in 2-methoxyethanol, **6** isomerizes to the species **6'** in which the carbonyl (ν(CO) 1981 cm⁻¹, KBr) is *cis* to both P atoms (*J*_{P,C} = 15.8 and 15.5 Hz). In the latter isomer, the ligand *trans* to CO is either an imine or Cl, but this cannot be assessed by IR data alone.²⁸

[RuCl(OH₂)(PNNP)]PF₆. The five-coordinate complexes **3a,b** react with most O-donors (L), such as H₂O, THF, CH₃OH, and diethyl ether, to give the corresponding adducts [RuCl(L)(PNNP)]⁺. As discussed above, the oxophilicity of the putative amino analogue **3c** is so high that only the aqua complex **5c** was ever detected. Thus, in view of the activation of hydrogen peroxide, the reactivity of **3a** and **3b** with water was investigated in detail. The binaphthyl analogue **3a** is the least reactive of the **3a–c** series. In the presence of water (1 equiv), it forms a species that is tentatively formulated as an aqua complex. The isolation of [RuCl(OH₂)(**1a**-κ⁴P,N,N,P)]PF₆ was not attempted, as the reaction is reversible and **3a** is reformed upon addition of molecular sieves to the solution.

In contrast, the reaction of **3b** with an excess of H₂O gives the stable aqua complex [RuCl(OH₂)(**1b**-κ⁴P,N,N,P)] (**5b**), which was isolated in the solid state and fully characterized. Bands at 3485 and 1602 cm⁻¹ in the IR spectrum are attributed to the O–H stretching and H–O–H bending, respectively. The molar conductivity (Λ_m = 39 Ω⁻¹ cm² mol⁻¹) and the ³¹P NMR signal of the uncoordinated [PF₆]⁻ anion indicates that the complex is an electrolyte in CH₂Cl₂ solution. In the ³¹P NMR spectrum, two AX systems featuring *cis* coupling constants (*J*_{P,P'} = 31.8 and 26.9 Hz) reveal that two different *cis* isomers are present, **5b'** (70%) and **5b''**

(30%). The isomer distribution is independent of the excess of water used in the synthesis and does not change upon heating the mixture of **5b'** and **5b''** for several hours (CDCl₃ at reflux). Complex **5b** does not dissociate the aqua ligand upon dissolution in dry solvents (CH₂Cl₂ or CHCl₃), even in the presence of molecular sieves. The coordinated water molecule is displaced by reaction of **5b** with HPF₆ in Et₂O, which quantitatively affords the ether adduct [RuCl(OEt₂)(**1b**-κ⁴P,N,N,P)]⁺. The latter can be independently prepared by addition of Et₂O (10 equiv) to **3b**.

Finally, the aqua derivative [RuCl(OH₂)(**1c**-κ⁴P,N,N,P)]PF₆ (**5c**) is apparently the last product of chloride abstraction from the dichloro complexes of ligand **1c** with Tl[PF₆]. Thus, complex **4** reacts with Tl[PF₆], giving **5c** and 1 equiv of PPh₃ (eq 2). In



addition, the reaction of the mixture of *cis*-β-**2c**, *trans*-**2c**, and **4** with Tl[PF₆] in CH₂Cl₂ gives **5c** instead of the putative five-coordinate [RuCl(**1c**-κ⁴P,N,N,P)]⁺. The characterization of **5c** was complicated by its limited stability in solution, as it decomposed during recrystallization. However, besides the analogy with **5b**, the formulation of **5c** as an aqua complex is supported by the molecular peak at *m/z* 817 in its FAB⁺ mass spectrum and by the fact that it does not react with an excess of water (in CDCl₃). The AX system in the ³¹P NMR spectrum indicates that **5c** is formed as a single isomer.

We never observed the putative reaction intermediate, the five-coordinate [RuCl(**1c**-κ⁴P,N,N,P)]PF₆ (**3c**), even when the reaction was carried out in rigorously dried solvents. As water can be present, at worst, only in traces under the reaction conditions employed (Schlenk techniques under argon, solvent distilled over CaH₂), we conclude that "[RuCl(**1c**-κ⁴P,N,N,P)]⁺" (**3c**) is the most oxophilic species of the **3a–c** series. As **5c** can be conveniently prepared by reacting the product mixture of **2c** and **4** with Tl[PF₆], we used this synthetic path (instead of the reaction with pure **4**) in the catalytic assays described below.

Aqua complexes of ruthenium(II) are common in combination with hard donors, such as in [Ru(OH₂)₂-(bipy)₂]ⁿ⁺²⁹ and in [Ru(OH₂)₆]²⁺.³⁰ In contrast, soft coligands, such as phosphines, disfavor water coordination at Ru(II), unless intramolecular H-bonding is possible, as in complexes with coordinated O-containing anions,³¹ or when a strong π-acceptor enhances the Lewis acidity, as in [RuCl₂(CO)(OH₂)(PET₃)₂].³² Aqua complexes stabilized by the combination of soft P donors and hard nitrogen ligands have already been reported, e.g. [Ru(OH₂)(PET₃)₂(terpy)₂]²⁺ and [Ru(OH₂)(dppe)-(Tp^{iPr})] (terpy = 2,2':6',2''-terpyridine; Tp^{iPr} = hydrido-

(29) Durham, B.; Wilson, S. R.; Hodgson, D. J.; Meyer, T. J. *J. Am. Chem. Soc.* **1980**, *102*, 600.

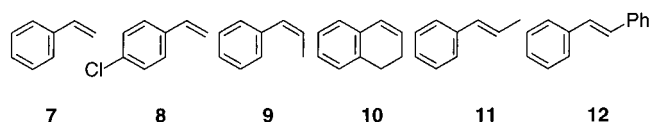
(30) Bernhard, P.; Bürgi, H. B.; Hauser, J.; Lehmann, H.; Ludi, A. *Inorg. Chem.* **1982**, *21*, 3936.

(31) (a) Mahon, M. F.; Whittlesey, M. K.; Wood, P. T. *Organometallics* **1999**, *18*, 4068. (b) Herold, S.; Mezzetti, A.; Venanzi, L. M.; Albinati, A.; Lianza, F.; Gerfin, T.; Gramlich, V. *Inorg. Chim. Acta* **1995**, *235*, 215.

(32) Sun, Y.; Taylor, N. J.; Carty, A. J. *Inorg. Chem.* **1993**, *32*, 4457.

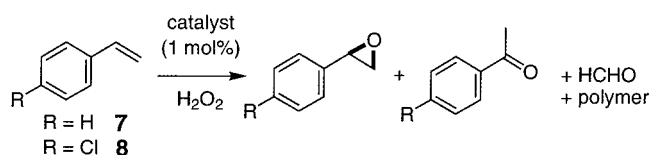
(28) See, for instance: (a) Ziesel, R.; Toupet, L.; Chardon-Noblat, S.; Deronzier, A.; Matt, D. *J. Chem. Soc., Dalton Trans.* **1997**, 3777. (b) Abbenhuis, R. A. T. M.; del Río, I.; Bergshoeff, M. M.; Boersma, J.; Veldman, N.; Spek, A. L.; van Koten, G. *Inorg. Chem.* **1998**, *37*, 1749.

Chart 5



tris(3,5-diisopropylpyrazolyl)borato).^{33,34} The aqua complexes $[\text{Ru}(\text{OH}_2)\text{L}_5]^{n+}$ are of particular interest, as their 2e oxidation can give oxo complexes of the type $[\text{Ru}^{\text{IV}}(\text{O})\text{L}_5]$, which have been used in a number of stoichiometric and catalytic oxygen-transfer reactions with alkanes,³⁵ alkenes,^{2c,36,37} alcohols,³⁸ phosphines,³⁹ and sulfides.⁴⁰ The electrochemistry of aqua complexes of ruthenium(II) has been investigated in great detail by Meyer,³⁷ Che,⁴¹ and Takeuchi.⁴² Thus, the aqua complex $[\text{RuCl}(\text{OH}_2)(\mathbf{1a}-\kappa^4\text{P,N,N,P})]^+$ (**3a**) is possibly related to the hypothetical ruthenium(IV) oxo species $[\text{RuCl}(\text{O})(\mathbf{1a}-\kappa^4\text{P,N,N,P})]^+$, the putative intermediate in the catalytic epoxidation described below. To this point, it is worth mentioning that we recently reported a related oxo complex of osmium(IV), $[\text{OsCl}(\text{O})(\text{dcpe})_2]^+$ (dcpe = 1,2-bis(dicyclohexylphosphino)ethane).⁴³

Asymmetric Epoxidation. The cationic complexes **3a,b** and **5b** were used as catalyst precursors for the enantioselective epoxidation of the unfunctionalized olefins in Chart 5 with hydrogen peroxide as oxidant. An alternative protocol exploits the generation of the catalyst in situ by reaction of the dichloro complexes **2a–c** with $\text{Ti}[\text{PF}_6]$. In the case of the amino ligand **1c**, this procedure yields the corresponding aqua derivative **5c**. In general, the dichloro complexes **2a–c** are catalytically inactive, and no reaction occurs either without the catalysts (**3a,b** and **5b,c**) or in the presence of the free ligand.⁴⁴ The reaction conditions were optimized using **3b** as catalyst and styrene as the substrate. The reaction products were quantified by gas chromatography, and enantiomeric excesses were determined by GC analysis on a chiral column. In a preliminary communication,¹⁷ we have reported the effect of a series of parameters, such as oxidant, solvent, temperature, and additives, on the reaction catalyzed by **3b** as precatalyst and styrene as substrate.

Table 2. Asymmetric Epoxidation of Styrenes^a

run	cat.	substr.	t (h)	conversion (%)	selectivity (%) ^b		ee ^d (%)
					epoxide	PhCHO	
1	3b	7	6	35	81	9	<i>S</i> 37
2	2b ^e	7	2	35	70	9	<i>S</i> 42
3	3b	8	4	25	60	5	nd 25
4	5b	7	6	39	68	9	<i>S</i> 30
5	5b	8	4	18	53	6	nd 12
6	5c ^e	7	2	20	12	17	<i>S</i> 40
7	3a ^e	7	6	18	7	27	<i>S</i> <5

^a Reaction conditions: olefin (0.96 mmol), catalyst (9.6 μmol), CH_2Cl_2 (5 mL), H_2O_2 (30%, 9.8 M, 6.68 mmol, 0.7 mL) added in one portion, 22 °C. ^b By GC analysis with decane as internal standard. ^c By comparison with an authentic sample (chiral GC analysis). ^d Determined by chiral GC (Supelco α -DEX 120). ^e Catalyst prepared in situ (see Experimental Section).

In the optimized procedure, aqueous hydrogen peroxide (30%, 7 equiv vs the olefin) is added in one portion to a CH_2Cl_2 solution containing styrene, the catalyst precursor (1 mol %), and decane as internal standard. Gas is evolved from the biphasic reaction system at the beginning of the reaction, apparently due to partial H_2O_2 decomposition. Gas evolution generally stops after 45 min of reaction time. For most olefins, oxidative cleavage of the C=C bond also occurs along with epoxide formation. Benzaldehyde is detected in the reaction mixture of acyclic olefins.

The epoxidation of styrene (**7**) in the presence of (*S,S*)-**3b** (1 mol %) and H_2O_2 (7 equiv vs **7**) gives (*S*)-styrene oxide with 81% selectivity and 37% ee after 6 h with 35% olefin conversion (Table 2, run 1). The oxidative cleavage of the C=C double bond is a minor side reaction, as only 9% of the initial styrene is converted to benzaldehyde after 6 h. The mass balance indicates that 10% of styrene forms products other than styrene oxide or benzaldehyde. The recovery of (atactic) polystyrene from the reaction mixture according to the mass balance shows that the loss of mass is due to polymerization of the olefin. The catalytic system can be also formed in situ by reacting the dichloro complex **2b** and $\text{Ti}[\text{PF}_6]$ in CH_2Cl_2 for 12 h. After filtration, the solution of the catalyst is added to a CH_2Cl_2 solution of the olefin and decane. This method gives 35% conversion after 2 h with 42% ee for styrene oxide, the highest value in this study (run 2).⁴⁵ Longer reaction times do not improve the conversion. In contrast to other systems, *p*-chlorostyrene (**8**) does not perform better than styrene (run 3).^{8e}

The aqua derivative **5b** is generally less efficient than **3b** (runs 4 and 5). This is rather surprising, as the use of aqueous H_2O_2 implies that the aqua complex **5b** must be present when **3b** is used as catalyst precursor. However, this effect could be related to the large number of diastereomers that these PNNP complexes can form

(33) Lawson, H. J.; Janik, T. S.; Churchill, M. R.; Takeuchi, K. J. *Inorg. Chim. Acta* **1990**, *174*, 197.

(34) Takahashi, Y.; Hikichi, S.; Akita, M.; Moro-oka, Y. *Organometallics* **1999**, *18*, 2571.

(35) Representative papers: (a) Groves, J. T.; Nemo, T. E. *J. Am. Chem. Soc.* **1983**, *105*, 6243. (b) Goldstein, A. S.; Drago, R. S. *J. Chem. Soc., Chem. Commun.* **1991**, 21. (c) Bailey, A. J.; Griffith, W. P.; Savage, P. D. *J. Chem. Soc., Dalton Trans.* **1995**, 3537.

(36) Representative papers: (a) Dobson, J. C.; Seok, W. K.; Meyer, T. J. *Inorg. Chem.* **1986**, *25*, 1513. (b) Che, C. M.; Li, C. K.; Tang, W. T.; Yu, W. Y. *J. Chem. Soc., Dalton Trans.* **1992**, 3153. (c) Goldstein, A. S.; Beer, R. H.; Drago, R. S. *J. Am. Chem. Soc.* **1994**, *116*, 2424.

(37) Stultz, L. K.; Binstead, R. A.; Reynolds, M. S.; Meyer, J. T. *J. Am. Chem. Soc.* **1995**, *117*, 2520 and references therein.

(38) Recent papers: (a) Catalano, V. J.; Heck, R. A.; Immoos, C. E.; Öhman, A.; Hill, M. G. *Inorg. Chem.* **1998**, *37*, 2150, and refs 1–7 therein. (b) Lebeau, E. L.; Meyer, T. J. *Inorg. Chem.* **1999**, *38*, 2174.

(39) Le Maux P.; Bahri, H.; Simonneaux, G.; Toupet, L. *Inorg. Chem.* **1995**, *34*, 4691.

(40) Hua, X.; Shang, M.; Lappin, A. G. *Inorg. Chem.* **1997**, *36*, 3735.

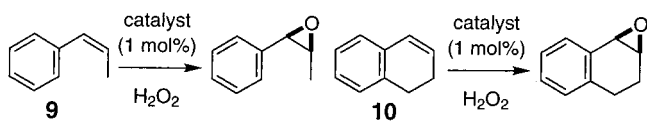
(41) Che, C. M.; Yam, V. W. W. In *Advances in Transition Metal Coordination Chemistry*; Che, C. M., Ed.; JAI Press: London, 1996; Vol. 1, p 209.

(42) Marmion, M. E.; Takeuchi, K. J. *J. Am. Chem. Soc.* **1988**, *110*, 1472.

(43) Barthazy, P.; Wörle, M.; Mezzetti, A. *J. Am. Chem. Soc.* **1999**, *121*, 480.

(44) Iminium salts have been found to catalyze the epoxidation of olefins: Ahmed, G.; Garnett, I.; Goacolou, K.; Wailes, J. S. *Tetrahedron* **1999**, *55*, 2341.

(45) To exclude the possibility that traces of TiCl_4 affect the catalytic results, we have studied the effect of added TiCl_4 . When TiCl_4 is not filtered off after the reaction of $\text{Ti}[\text{PF}_6]$ with $[\text{RuCl}_2(\mathbf{1b}-\kappa^4\text{P,N,N,P})]$, the reaction gives results analogous to those of run 1 (25% conversion, 28% selectivity for the epoxide after 6 h). No oxidation occurs in the presence of TiCl_4 (1 mol %) and without the metal complex.

Table 3. Asymmetric Epoxidation of *cis*-Olefins^a


run	cat.	substr	<i>t</i> (h)	conversn (%)	selectivity (%)		ee ^b (%)
					epoxide	other	
1	3b	9	2	22	72	<i>c</i>	25 ^d
2	5b	9	2	6	70	<i>c</i>	22 ^e
3	3b	10	2	100	55	<i>f</i>	41
4 ^b	3b	10	2	100	53	<i>f</i>	39
5	5b	10	2	100	50	<i>f</i>	25
6	5c ⁱ	10	1	78	55	<i>f</i>	29
7	3a	10	2	15	4	<i>f</i>	<5

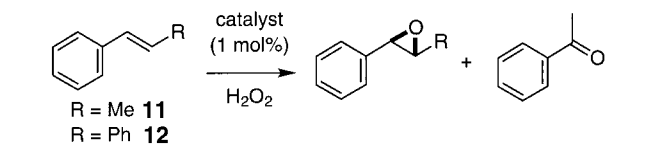
^a See Table 2 (footnote a) for reaction and analytical conditions.^b Determined by chiral GC (Supelco α-DEX 120). ^c Traces of *trans* epoxide are detected (*cis:trans* ratio is 99:1). ^d ee of *trans* isomer is 38%. ^e ee of *trans* isomer is 23%. ^f Overoxidation products have been detected by GC MS (see text). ^g By the sign of the optical rotation. ^h Substrate:catalyst ratio is 200. ⁱ Catalyst prepared in situ (see Experimental Section).

(see below). The amino ligand **1c**, tested with the in situ procedure described above, gives much lower epoxide selectivity (run 6) than the complexes with the imino ligand **1b**. The mass balance suggests that this is due to olefin polymerization. Finally, the binaphthylene ligand **1a** gives the lowest enantioselectivity and epoxide selectivity (run 7). Again, the missing mass can be explained with the competing polymerization of the olefin.

The epoxidation of (*Z*)-2-methylstyrene (**9**) catalyzed by complex **3b** gives the *cis*-epoxide as the main product and only traces of *trans*-epoxide (the *cis:trans* ratio is 99:1) (Table 3, run 1). The enantioselectivities of the *cis* and *trans* epoxides are 25% and 38% ee, respectively. The aqua complex **5b** gives similar selectivity, but much lower conversion (run 2). The stereospecificity of the epoxidation reaction catalyzed by **3b** and **5b** is much higher than that observed in Mn-catalyzed epoxidations of *cis*-disubstituted olefins.⁴ Within the assumption that the catalytic cycle involves an oxo species, this stereospecificity suggests concerted oxene transfer to the double bond.^{1,6}

With **3b** as catalyst precursor, the *cis*-constrained olefin 1,2-dihydronaphthalene (**10**) is quantitatively converted after 2 h, forming the (–)-(1*S*,2*R*)-epoxide with 55% selectivity and 41% ee (Table 3, run 3). Minor amounts of 1,2-dihydroxy-3,4-dihydronaphthalene and 1-oxo-2,3,4-trihydronaphthalene are detected by GC MS among the reaction products. Quantitative conversion of **10** is obtained also with a substrate to catalyst ratio of 200:1 (run 4). The aqua complex **5b** shows similar activity and chemoselectivity, but the ee is lower (25%, run 5), and the amino analogue **5c** gives both lower ee (29%) and lower conversion (78%) than **3b** (run 6). With **5c**, the epoxide selectivity drops during the reaction: monitoring by GC shows that the epoxidation reaction stops at 78% conversion of **10** after 1 h with 55% epoxide selectivity. After 2 h of reaction time, the selectivity for the epoxide drops to 4%. GC-MS analysis indicates that the epoxide decomposes to the dialdehyde. Eventually, no epoxide is observed after 6 h of reaction time.

We tested *trans*-β-methylstyrene (**11**) and *trans*-stilbene as models of *trans*-disubstituted olefins. Complex **3b** gives nearly racemic epoxide with **11** (4% ee),

Table 4. Asymmetric Epoxidation of *trans*-Olefins^a


run	cat.	substr	<i>t</i> (h)	conversn (%)	selectivity (%)		ee ^b (%)
					epoxide	RCHO	
1	3b	11	2	26	62	17	4
2	5b	11	2	14	52	4	10
3	3b	12	4	45	69	0	12
4	5b	12	4	14	65	0	12

^a See Table 2 (footnote a) for reaction and analytical conditions.^b Determined by chiral GC (Supelco α-DEX 120). ^c By comparison with an authentic sample (chiral GC analysis).

with conversion and selectivity comparable to those of styrene (Table 4, run 1). The aqua complex **5b** is less active, but some enantioselectivity is observed (run 2). Similarly, *trans*-stilbene gives moderate conversion and chemoselectivity, together with low ee values (runs 3 and 4).

Finally, we investigated the fate of the catalyst **3b** upon addition of H₂O₂ to check the stability of the coordinated phosphine ligands toward oxidation. Aqueous H₂O₂ (30%, 1 equiv) was layered over a CDCl₃ solution of **3b**, and the reactions occurring upon diffusion into the organic phase were monitored by ³¹P and ¹H NMR spectroscopy. After 10 min, the solution contains equal amounts of starting **3b** and of aqua complex **5b** (by integration of the ³¹P NMR signals). Interestingly, only the isomer **5b'** is observed. After 90 min, the signals of **3b** have disappeared, and the signal of aqua complex **5b'** is present along with those of unidentified products at δ 36 (m), 31.9 (s), and 30.0 (s). Integration of the ³¹P spectrum indicates that **5b'** is about 50% of total. After 48 h, **5b'** has apparently reacted to give an unidentified species having ³¹P NMR signals in the δ range 30–40. On the basis of chemical shifts and multiplicity, the latter compounds could be metal complexes containing coordinated phosphine oxides,⁴⁶ whose nature will be the subject of future investigations. In conclusion, the formation of aqua derivative **5b'** is the fastest reaction in solution and is followed by a reaction that probably involves oxidation of the phosphine arms.

This result gives some clue regarding the catalytic reaction. As we generally observe vigorous gas evolution immediately after addition of H₂O₂, we believe that the complex itself (rather than decomposition products thereof) decomposes H₂O₂. Decomposition of H₂O₂ by transition-metal compounds is a very general reaction. It can occur with a catalase mechanism if a Ru=O species is involved. Alternatively, traces of Ru(III) can start a Fenton process.³ Also, the observation of one single isomer of the aqua complex **5b** as the kinetic product of H₂O addition to **3b** offers an explanation for the different reactivities observed with **3b** and **5b**. In fact, the catalytic experiments were performed with the isolated aqua complex containing a mixture of diastereomers **5b'** and **5b''**, which might have different catalytic behavior.

(46) See, for instance: (a) Jia, G.; Ng, W. S.; Chu, H. S.; Wong, W. T.; Yu, N. T.; Williams, I. D. *Organometallics* **1999**, *18*, 3602. (b) Maj, A. M.; Pietrusiewicz, K. M.; Suisse, I.; Agbossou, F.; Mortreux, A. *Tetrahedron: Asymmetry* **1999**, *10*, 831.

To the best of our knowledge, this is the first asymmetric epoxidation catalyzed by a ruthenium complex that exploits hydrogen peroxide as oxidant.⁴⁷ With the exception of 1,2-dihydronaphthalene, the olefin conversion is moderate (up to 45% for **12**), and the decomposition of hydrogen peroxide occurs parallel to epoxidation. However, the relatively small excess of H₂O₂ used (7 equiv vs olefin) is worthy of note, as transition-metal complexes efficiently decompose H₂O₂.³ Most interestingly, the system activity is up to a TOF of 18 h⁻¹ (Table 2, run 2), which is an order of magnitude larger than for ruthenium systems containing N- or N,O-donor ligands.⁹ The high activity of the complexes [RuCl(PNNP)]⁺ explains why the catalytic epoxidation reaction effectively competes with the decomposition of the oxidant. A general feature of the above reactions is the high chemoselectivity, with selectivity for epoxide formation as high as 81%. This is better than that observed with other ruthenium-based catalytic systems, which generally afford substantial amounts of cleavage products.^{11,15,16,48}

Conclusion

We have shown that new cationic ruthenium complexes containing tetradentate chiral ligands with a P₂N₂ donor set are effective catalysts for the asymmetric epoxidation of alkenes with hydrogen peroxide. Clearly, chloride abstraction is necessary to catalytic activity, as the dichloro species [RuCl₂(PNNP)] are catalytically inactive under the same conditions. In particular, H₂O₂ is activated with high efficiency, which points to the role played by the high oxophilicity of the five-coordinate complexes. Indeed, best results are obtained with **3b**, which forms the stable aqua complex **5b**. Either reduced oxophilicity (as in **3a**) or reduced stability of the aqua complex (as in **5c**) decreases the efficiency of the system. The stereospecificity of the epoxidation reaction suggests that the intermediates involved have little radical character.

Experimental Section

General Considerations. Reactions with air- or moisture-sensitive materials were carried out under an argon atmosphere using Schlenk techniques. Styrene, 1,2-dihydronaphthalene, *rac*-styrene oxide, (*R*)-styrene oxide, and (1*S*,2*S*)-(+)-1,2-diaminocyclohexane were obtained from Fluka AG. *trans*- β -Methylstyrene, (1*R*,2*R*)-*trans*- β -methylstyrene oxide, and 2-(diphenylphosphino)benzaldehyde were purchased from Aldrich; Ti[PF₆] was obtained from Strem Chemicals. [RuCl₂(PPh₃)₃], *cis*- β -methylstyrene, *rac*-1,2-dihydronaphthalene oxide, *rac*-*trans*- β -methylstyrene oxide, and *rac*-*cis*- β -methylstyrene oxide were prepared according to literature procedures (see the Supporting Information). NMR spectra were recorded on Bruker AVANCE spectrometers. ¹H and ¹³C positive chemical shifts in ppm are downfield from tetramethylsilane. ³¹P NMR spectra were referenced against external 85% H₃PO₄. The diffusion measurements were performed on a Bruker AVANCE 400 spectrometer equipped

with a microprocessor-controlled gradient unit and a multinuclear probe with an actively shielded Z-gradient coil. The complexes were dissolved in distilled CDCl₃ and measured at 296 K without spinning. The shape of the gradients was rectangular; their length (δ) was 5 ms, the strength (G) was varied in the course of the experiments, from 0.56 to 24.08 G cm⁻¹, every 0.56 G cm⁻¹, and the diffusion time (Δ) was equal to 66 ms.

Mass spectra were measured by the MS service of the Laboratorium für Organische Chemie (ETH Zürich). A 3-NO-BA (3-nitrobenzyl alcohol) matrix and a Xe atom beam with a translational energy of 8 keV were used for FAB⁺ MS. Optical rotations were measured using a Perkin-Elmer 341 polarimeter with a 1 dm cell. Elemental analyses were carried out by the Laboratory of Microelemental Analysis (ETH Zürich).

***N,N*-Bis[α -(diphenylphosphino)benzylidene]-2,2'-diimino-1,1'-(*S*)-binaphthylene (**1a**).** (*S*)-(-)-2,2'-Diamino-1,1'-binaphthalene (257 mg, 0.905 mmol) and 2-(diphenylphosphino)benzaldehyde (522 mg, 1.810 mmol) were stirred in toluene (15 mL) at room temperature for 14 h. The resulting yellow solution was refluxed in a Dean-Stark apparatus for 2 h. Evaporation of the solvent under vacuum and recrystallization of the resulting yellow oil from MeOH/toluene (4:1) gave a yellow solid. Yield: 700 mg (94%). $[\alpha]_D^{20}$: -126.4 \pm 2° (c = 1). ¹H NMR (250 MHz, CDCl₃): δ 8.9 (d, 2H, H -C=N, $J_{P,H}$ = 6 Hz), 7.85 (m, 2H, arom), 7.55–6.8 (m, 36H, arom), 6.6 (m, 2H, arom). ³¹P NMR (101 MHz, CDCl₃): δ -15.2 (s) (δ -16.5 was reported for (*rac*)-**1c**).¹⁸ MS (EI): m/z 829 (M⁺, 98), 751 ([M - Ph]⁺, 40), 540 ([M - N=C-PPh₂]⁺, 100). Other analytic and spectral data are as in ref 20.

***N,N*-Bis[α -(diphenylphosphino)benzylidene]-(1*S*,2*S*)-diiminocyclohexane ((*S,S*)-**1b**).** (1*S*,2*S*)-(+)-1,2-Diaminocyclohexane (63 mg, 0.54 mmol) and 2-(diphenylphosphino)benzaldehyde (317 mg, 1.08 mmol) were dissolved in toluene (10 mL), and the resulting orange-yellow solution was stirred for 10 h at room temperature. Then, the reaction solution was heated to reflux in a Dean-Stark apparatus, after which toluene was evaporated. The resulting yellow oil was recrystallized from toluene/MeOH to give a white solid. Yield: 320 mg (90%). $[\alpha]_D^{23}$: -74.9 \pm 0.2° (CHCl₃, c = 1). ¹H NMR (250 MHz, CDCl₃): δ 8.7 (d, 2H, N=CH), 7.7 (m, 2H, arom), 7.3–7.15 (m, 24H, arom), 6.8 (m, 2H, arom), 3.1 (m, 2H, N-CH), 1.2–1.7 (m, 8 H, CH₂). ³¹P NMR (101 MHz, CDCl₃): δ -13.9 (s, 2P). IR (KBr, cm⁻¹): 1635 (s, ν_{CN}). MS (EI): m/z 658 (M⁺, 2), 581 ([M - Ph]⁺, 42), 288 ([M - 2PPh₂]⁺, 100). Anal. Calcd for C₄₄H₄₀N₂P₂: C, 80.22; H, 6.12; N, 4.25. Found: C, 80.16; H, 6.38; N, 4.29.

***N,N*-Bis[α -(diphenylphosphino)benzylidene]-(1*S*,2*S*)-diaminocyclohexane ((*S,S*)-**1c**).** Ligand **1b** (1.00 g, 1.52 mmol) and NaBH₄ (608 mg, 16 mmol) were refluxed for 24 h in ethanol (100 mL). The solution was cooled, and the solvent was removed under vacuum. The resulting solid was suspended in CH₂Cl₂ (70 mL) and filtered over Celite. The solvent was removed under vacuum, and the resulting creamy solid was recrystallized from CH₂Cl₂/hexane. Yield: 674 mg (67%). ¹H NMR (250 MHz, CDCl₃): δ 7.58–7.53 (m, 4 H, arom), 7.34–7.13 (m, 22 H, arom), 6.87–6.82 (m, 2 H, arom), 4.15 (d, 2 H, PhCH₂N, $J_{H,H'} = 13.4$ Hz), 3.91 (d, 2 H, PhCH₂N, $J_{H,H'} = 13.4$), 2.4 (br, 1 H, N-CH), 2.05 (br, 1 H, N-CH), 1.67 (br, 2H, NH), 1.47–1.04 (m, 8 H, Cy H). ³¹P NMR (101 MHz, CDCl₃): -15.9 (s, 2P). Other analytic and spectral data are as in ref 18.

[RuCl₂(1a- κ^4 P,N,N,P)] (2a**).** Ligand **1a** (511 mg, 0.78 mmol) and [RuCl₂(PPh₃)₃] (743.2 mg, 0.78 mmol) were stirred in CH₂Cl₂ (10 mL) for 14 h, after which hexane (50 mL) was added. When the solution was concentrated, red microcrystals precipitated, which were filtered off, washed with hexane, and dried under vacuum. Recrystallization was from CH₂Cl₂/hexane. Yield: 668 mg (86%). This procedure gives a mixture of two different *cis*- β isomers (50 and 40%) and a *trans* isomer (10%). ¹H NMR (250 MHz, CDCl₃): *cis*- β -**2a'** (50%), δ 8.4 (d, 1

(47) We did not attempt to develop a mechanistic interpretation of enantioselection, since the (hypothetical) oxo intermediate [RuCl(O)-(PNNP)] can be formed in seven diastereomers (one *trans*, four *cis*- β , and two *cis*- α isomers). The analysis of the 14 transition states is a daunting task, also in view of the low energy differences between them, as indicated by the moderate to low enantioselectivity.

(48) Augier, C.; Malara, L.; Lazzeri, V.; Waegell, B. *Tetrahedron Lett.* **1995**, *36*, 8775.

H, $J_{\text{P,H}} = 8.3$ Hz, $\text{N}=\text{CH}$), 8.3 (s, 1 H, arom), 8.1–6.4 (m, 37 H, arom), 5.63 (d, 1 H, $J_{\text{P,H}} = 8.6$ Hz, $\text{N}=\text{CH}$), 5.24 (m, 2 H, arom); *cis*- β -**2a''** (40%), δ 8.4 (d, 1 H, $J_{\text{P,H}} = 8.3$ Hz, $\text{N}=\text{CH}$); *trans*-**2a** (10%), δ 8.55 (d, 2 H, $J_{\text{P,H}} = 6.1$ Hz, $\text{N}=\text{CH}$). ^{31}P NMR (101 MHz, CDCl_3): *cis*- β -**2a'**, δ 49.4 (d, 1P, $J_{\text{P,P'}} = 31.9$ Hz), 41.4 (d, 1P, $J_{\text{P,P'}} = 31.9$ Hz); *cis*- β -**2a''**, δ 52.3 (d, 1P, $J_{\text{P,P'}} = 33.5$ Hz), 43.5 (d, 1P, $J_{\text{P,P'}} = 33.5$ Hz); *trans*-**2a**, δ 46.4 (s, 2P). MS (FAB⁺): m/z 1001 ($[\text{M} + 1]^+$, 10), 1000 (M^+ , 13), 966 ($[\text{M} + 1 - \text{Cl}]^+$, 75), 965 ($[\text{M} - \text{Cl}]^+$, 100). Anal. Calcd for $\text{C}_{58}\text{H}_{42}\text{N}_2\text{P}_2\text{Cl}_2\text{Ru} \cdot 0.5\text{CH}_2\text{Cl}_2$: C, 67.34; H, 4.15; N, 2.68. Found: C, 67.53; H, 4.85; N, 2.72. The minor *cis* isomer *cis*- β -**2a''** was separated from *cis*- β -**2a'** and *trans*-**2a** by column chromatography over alumina with CH_2Cl_2 /hexane (1:1) as eluent.

[RuCl(1a- $\kappa^4\text{P,N,N,P}$)]PF₆ (3a). **[RuCl₂(1a- $\kappa^4\text{P,N,N,P}$)]** (373 mg, 0.37 mmol) and $\text{Ti}[\text{PF}_6]$ (131 mg, 0.37 mmol) were stirred for 16 h in CH_2Cl_2 (20 mL). After filtration of TiCl_4 over Celite, pentane (50 mL) was added. Partial evaporation of the solvent yielded a purple precipitate, which gave red-brown microcrystals after recrystallization from CH_2Cl_2 /pentane. Yield: 282 mg (69%). ^1H NMR (300 MHz, CDCl_3): δ 8.84 (d, 1 H, $\text{N}=\text{C}-\text{H}$, $J_{\text{P,H}} = 9.6$ Hz), 8.60 (s, 1 H, arom), 8.25 (d, 1 H, arom, $J_{\text{H,H'}} = 8.6$ Hz), 8.08 (m, 2 H, arom), 7.9–6.4 (m, 36 H, arom), 4.94 (d, 1 H, $\text{N}=\text{C}-\text{H}$, $J_{\text{P,H}} = 8.6$ Hz). ^{31}P NMR (250 MHz, CDCl_3): δ 79.8 (d, 1P, $J_{\text{P,P'}} = 27.6$ Hz), 44.5 (d, 1P, $J_{\text{P,P'}} = 27.6$ Hz). MS (FAB⁺): m/z 965 (M^+ , 100), 930 ($[\text{M} - \text{Cl}]^+$, 10). Anal. Calcd for $\text{C}_{58}\text{H}_{42}\text{N}_2\text{F}_6\text{P}_3\text{ClRu} \cdot 0.25\text{CH}_2\text{Cl}_2$: C, 61.82; H, 3.79; N, 2.48. Found: C, 61.61; H, 4.07; N, 2.69.

[RuCl₂(1b- $\kappa^4\text{P,N,N,P}$)] (2b). **[RuCl₂(PPh₃)₃]** (282 mg, 0.294 mmol) and **1b** (194 mg, 0.294 mmol) were dissolved in CH_2Cl_2 (30 mL), and the resulting brown solution was stirred at room temperature for 4 h. Addition of hexane and partial evaporation of the solvent gave a bordeaux red solid. Yield: 223 mg (91%). ^1H NMR (250 MHz, CDCl_3): *cis*- β -**2b** (20%), δ 8.96 (d, 1H, $J_{\text{P,H}} = 10.2$ Hz, $\text{N}=\text{CH}$); *trans*-**2b** (80%), δ 8.90 (d, 2H, $J_{\text{P,H}} = 8.7$ Hz, $\text{N}=\text{CH}$), 7.68–6.51 (m, 28H, arom), 4.18 (d, 2H, $\text{N}-\text{CH}$, $J_{\text{H,H'}} = 8.2$ Hz), 2.72 (d, 2H, cyclohexyl- CH_2 , $J_{\text{H,H'}} = 11.6$ Hz), 2.06 (m, 2H, cyclohexyl- CH_2), 1.42 (m, 4H, cyclohexyl- CH_2). ^{31}P NMR (101 MHz, CDCl_3): *cis*- β -**3**, 88.3 (d, 1P, $J_{\text{P,P'}} = 31.7$ Hz), 36.1 (d, 1P, $J_{\text{P,P'}} = 31.7$ Hz); *trans*-**2b**, 47.7 (s, 2P). MS (FAB⁺): m/z 830 (M^+ , 100), 795 ($[\text{M} - \text{Cl}]^+$, 54), 759 ($[\text{M} - 2\text{Cl}]^+$, 10). Anal. Calcd for $\text{C}_{44}\text{H}_{40}\text{Cl}_2\text{N}_2\text{P}_2\text{Ru}$: C, 63.62; H, 4.85; N, 3.37. Found: C, 63.46; H, 4.90; N, 3.13.

[RuCl(1b- $\kappa^4\text{P,N,N,P}$)]PF₆ (3b). Complex **2b** (244 mg, 0.294 mmol) and $\text{Ti}[\text{PF}_6]$ (124 mg, 0.352 mmol) were stirred at room temperature in CH_2Cl_2 (30 mL) for 3 h. After filtration over Celite and addition of hexane, evaporation of CH_2Cl_2 yielded a red-brown solid. Yield: 204 mg (74%). ^1H NMR (250 MHz, CD_2Cl_2 , over molecular sieves): δ 8.85 (d, 1 H, $J_{\text{P,H}} = 10.0$ Hz, $\text{N}=\text{CH}$), 8.6 (br s, 1 H, $\text{N}=\text{CH}$). ^{31}P NMR (101 MHz, CD_2Cl_2 , over molecular sieves): δ 59.0 (d, 1P, $J_{\text{P,P'}} = 28.2$ Hz), 49.7 (d, $J_{\text{P,P'}} = 28.2$ Hz, 1P), –144.4 (septet, 1P, $J_{\text{P,P'}} = 714$ Hz, PF_6). $\Delta_M = 40 \text{ } \Omega^{-1} \text{ cm}^2 \text{ mol}^{-1}$ ($10^{-3} \text{ mol dm}^{-3}$ CH_2Cl_2 solution). MS (FAB⁺): m/z 796 ($[\text{M} + \text{H}]^+$, 100), 760 ($[\text{M} - \text{Cl}]^+$, 17).

Attempted Synthesis of *cis*- β -[RuCl₂(1c- $\kappa^4\text{P,N,N,P}$)] (2c). Ligand **1c** (971 mg, 1.467 mmol) and **[RuCl₂(PPh₃)₃]** (1.467 g, 1.467 mmol) were stirred in CH_2Cl_2 (70 mL) for 14 h. After it was refluxed for an additional 24 h, the solution was cooled, and hexane was added. Partial evaporation of the solvent under vacuum gave a brown solid, which was filtered off, washed with hexane, and dried under vacuum. Recrystallization from CH_2Cl_2 /hexane yielded a 6:3:1 mixture of **4**, *cis*- β -**2c**, and *trans*-**2c**. Yield: 942 mg (ca. 65%). ^{31}P NMR (101 MHz, CDCl_3): **4** (60%), δ 45.8 (d, 1P, $J_{\text{P,P'}} = 29.4$ Hz), 38.0 (d, 1P, $J_{\text{P,P'}} = 29.4$ Hz); *cis*- β -**2c** (30%), δ 54.0 (d, 1P, $J_{\text{P,P'}} = 28.7$ Hz), 37.3 (d, 1P, $J_{\text{P,P'}} = 28.7$ Hz); *trans*-**2c** (10%), δ 42.5 (s, 2P). See below for data of **4**. MS (FAB⁺): m/z 1096 (M^+ , 9, **4**), 834 (M^+ , 100, **2c**), 799 ($[\text{M} - \text{Cl}]^+$, 11, **2c**), 761 ($[\text{M} - 2\text{Cl} - 3\text{H}]^+$, 93, **2c**), 263 ($[\text{PPh}_3\text{H}]^+$, 42, from **4**). Column chromatography of the reaction mixture (alumina, CH_2Cl_2 /hexane (1:1))

yielded pure **4** and a mixture of *trans*-**2c** and *cis*- β -**2c**. Data for orange-red **4** are as follows. ^{31}P NMR (250 MHz, CDCl_3): δ 45.8 (d, 1P, PNNP coord), 38.8 (d, 1P, PPh_3), –14.7 (s, 1P, dangling PNNP). MS (FAB⁺): m/z 1096 (M^+ , 60), 834 ($[\text{M} - \text{PPh}_3]^+$, 100), 799 ($[\text{M} - \text{PPh}_3 - \text{Cl}]^+$, 27), 764 ($[\text{M} - \text{PPh}_3 - 2\text{Cl}]^+$, 15). Anal. Calcd for $\text{C}_{62}\text{H}_{59}\text{Cl}_2\text{N}_2\text{P}_3\text{Ru} \cdot \text{CH}_2\text{Cl}_2$: C, 64.02; H, 5.20; N, 2.37. Found: C, 63.57; H, 5.41; N, 2.45.

X-ray Analysis of [RuCl₂(PPh₃)(1c- $\kappa^3\text{P,N,N}$)] (4). Red crystals of **4** were grown from CH_2Cl_2 /PrⁱOH. A needle ($0.60 \times 0.06 \times 0.02$ mm) was mounted on a glass capillary. Crystal data for $\text{C}_{63}\text{H}_{61}\text{Cl}_4\text{N}_2\text{P}_3\text{Ru}$: orthorhombic, $P2_12_12_1$, cell dimensions (298 K) $a = 10.3532(2)$ Å, $b = 17.6566(3)$ Å, $c = 31.6328(3)$ Å, and $V = 5782.6(2)$ Å³ with $Z = 4$ and $D_c = 1.358 \text{ Mg/m}^3$, $\mu = 0.580 \text{ mm}^{-1}$ (Mo K α , graphite monochromated), $\lambda = 0.71073$ Å, $F(000) = 2440$. The data were collected at room temperature on a Siemens SMART platform in the θ range 1.29–20.82°. The structure was solved with SHELXTL using direct methods. Of the 25 499 measured reflections with index ranges $-10 \leq h \leq 10$, $-17 \leq k \leq 15$, and $-31 \leq l \leq 31$, and 6061 independent reflections, 4677 reflections with $I > 2\sigma(I)$ were used in the refinement (full-matrix least squares on F^2 with anisotropic displacement parameters for all non-H atoms). Hydrogen atoms were introduced at calculated positions and refined with the riding model and individual isotropic thermal parameters for each group. Final residuals were $R1 = 0.0657$ ($I > 2\sigma(I)$), $R1 = 0.0993$ (all 6061 reflections), $wR2 = 0.1404$ (all data), $\text{GOF} = 1.133$. Maximum and minimum difference peaks were +0.55 and –0.44 e Å^{–3}; largest and mean $\Delta/\sigma = -0.004$ and 0.000. Atomic coordinates, anisotropic displacement coefficients, and an extended list of interatomic distances and angles are available as Supporting Information. Selected interatomic distances and angles are reported in Table 1.

[RuCl(CO)(1b- $\kappa^4\text{P,N,N,P}$)]PF₆ (6). Complex **2b** (100 mg, 0.104 mmol) and $\text{Ti}[\text{PF}_6]$ (44 mg, 0.125 mmol) were dissolved in CH_2Cl_2 (10 mL). The red solution was stirred for 3 h at room temperature and then filtered over Celite and saturated with CO gas. Addition of hexane to the resulting orange solution and partial evaporation of the solvent yielded a yellow precipitate. Yield: 88 mg (87%). ^1H NMR (250 MHz, CDCl_3): δ 8.92 (s, 1H, $\text{N}=\text{CH}$), 8.64 (d, 1H, $\text{N}=\text{CH}$, $J_{\text{P,H}} = 9.4$ Hz), 8.24–6.41 (m, 28H, arom), 2.79 (m, 1H, $\text{N}-\text{CH}$), 2.52 (m, 1H, $\text{N}-\text{CH}$), 1.94 (m, 2H, CH_2), 1.36–1.21 (m, 6H, CH_2). ^{31}P NMR (101 MHz, CDCl_3): δ 35.0 (d, 1P, $J_{\text{P,P'}} = 28.8$ Hz), 22.6 (d, 1P, $J_{\text{P,P'}} = 28.2$ Hz), –144.4 (septet, 1P, $J_{\text{P,P'}} = 714$ Hz, PF_6). ^{13}C NMR (75 MHz, CDCl_3): δ 194.8 (dd, 1C, $J_{\text{P,C}} = 110.0$ Hz, $J_{\text{P,C}} = 15.1$ Hz, CO). IR (KBr, cm^{–1}): 2016 (s, ν_{CO}), 1640 (m, ν_{CN}). MS (FAB⁺): m/z 824 (M^+ , 28), 795 ($[\text{M} - \text{CO}]^+$, 100). Anal. Calcd for $\text{C}_{45}\text{H}_{40}\text{N}_2\text{OF}_6\text{P}_3\text{ClRu}$: C, 55.82; H, 4.16; N, 2.89. Found: C, 55.56; H, 4.57; N, 2.84.

[RuCl(H₂O)(1b- $\kappa^4\text{P,N,N,P}$)]PF₆ (5b). Complex **2b** (302 mg, 0.363 mmol) and $\text{Ti}[\text{PF}_6]$ (165 mg, 0.471 mmol) were dissolved in CH_2Cl_2 (40 mL). The red solution was stirred for 3 h at room temperature and then filtered over Celite into a PrⁱOH–H₂O (1:1) solution. Partial evaporation of the solvent yielded a yellow-orange solid. Yield: 288 mg (83%). ^1H NMR (250 MHz, CDCl_3): isomer **5b'** (70%), δ 8.80 (d, $J_{\text{P,H}} = 10.2$ Hz, 1H, $\text{N}=\text{CH}$), 8.68 (br s, 1H, $\text{N}=\text{CH}$); isomer **5b''** (30%), δ 9.21 (d, $J_{\text{P,H}} = 9.0$ Hz, 1H, $\text{N}=\text{CH}$), 8.88 (d, $J_{\text{P,H}} = 9.0$ Hz, 1H, $\text{N}=\text{CH}$). ^{31}P NMR (101 MHz, CDCl_3): isomer **5b'**, δ 65.0 (d, $J_{\text{P,P'}} = 31.8$ Hz, 1P), 45.5 (d, $J_{\text{P,P'}} = 31.8$ Hz, 1P); isomer **5b''**, 42.9 (d, $J_{\text{P,P'}} = 26.9$ Hz, 1P), 50.9 (d, $J_{\text{P,P'}} = 26.9$ Hz, 1P), –144.4 (septet, $J_{\text{P,P'}} = 714$ Hz, 1P, PF_6). IR (CHCl₃): $\nu_{\text{OH}} = 3685, 3604, 3485$ (br) cm^{–1}; $\nu_{\text{CN}} = 1630, 1602$ cm^{–1}. $\Delta_M = 39 \text{ } \Omega^{-1} \text{ cm}^2 \text{ mol}^{-1}$ ($10^{-3} \text{ mol dm}^{-3}$ CD_2Cl_2 solution). MS (FAB⁺): m/z 813 (M^+ , 10), 795 ($[\text{M} - \text{H}_2\text{O}]^+$, 100), 759 ($[\text{M} - \text{Cl} - \text{H}_2\text{O}]^+$, 24). Anal. Calcd for $\text{C}_{44}\text{H}_{42}\text{ClF}_6\text{N}_2\text{OP}_3\text{Ru}$: C, 55.15; H, 4.42; N, 2.92. Found: C, 55.83; H, 4.94; N, 2.37.

[RuCl(H₂O)(1c- $\kappa^4\text{P,N,N,P}$)]PF₆ (5c). A mixture of **2c** and **4** (227 mg, ca. 0.23 mmol) and $\text{Ti}[\text{PF}_6]$ (94 mg, 0.27 mmol) were dissolved in CH_2Cl_2 (10 mL). The brown solution was stirred

for 12 h at room temperature and then filtered over Celite into a $\text{Pr}^i\text{OH}-\text{H}_2\text{O}$ (1:1) solution. Partial evaporation of the solvent yielded a yellow-orange solid. Yield: 125 mg (ca. 67%). The complex decomposes to unidentified products upon recrystallization from $\text{CH}_2\text{Cl}_2/\text{hexane}$. ^{31}P NMR (101 MHz, CDCl_3): δ 65.8 (d, $J_{\text{P,P}'} = 31.9$ Hz, 1P), 45.8 (d, $J_{\text{P,P}'} = 31.9$ Hz, 1P), -144.4 (septet, $J_{\text{PF}} = 714$ Hz, 1P, PF_6). MS (FAB^+): m/z 817 (M^+ , 16), 800 ($[\text{M} - \text{H}_2\text{O}]^+$, 79), 763 ($\text{M} - \text{Cl} - \text{H}_2\text{O} - \text{H}]^+$, 100).

[RuCl(L)(1b- $\kappa^4\text{P,N,N,P}$)]PF₆. The [RuCl(L)(1b- $\kappa^4\text{P,N,N,P}$)]PF₆ adducts with L = Et₂O, THF, MeOH, and CH₃CN were prepared as follows: [RuCl(1b- $\kappa^4\text{P,N,N,P}$)]PF₆ (15 mg, 16 mmol) was dissolved under argon in CD_2Cl_2 (0.5 mL) or CDCl_3 , and L (10 equiv) was added with a microsyringe. ^{31}P NMR (101 MHz, CDCl_3): Et₂O (CD_2Cl_2), δ 64.0 (d, 1P, $J_{\text{P,P}'} = 30.1$ Hz), 48.2 (d, 1P, $J_{\text{P,P}'} = 30.1$ Hz); THF (CD_2Cl_2), δ 61.3 (d, 1P, $J_{\text{P,P}'} = 32.5$), 43.5 (d, 1P, $J_{\text{P,P}'} = 32.5$); MeOH (CD_2Cl_2), δ 61.5 (d, 1P, $J_{\text{P,P}'} = 32.5$), 43.5 (d, 1P, $J_{\text{P,P}'} = 32.5$); CH₃CN (CDCl_3), δ 48.5 (d, 1P, $J_{\text{P,P}'} = 26.6$), 42.2 (d, 1P, $J_{\text{P,P}'} = 26.6$).

Catalytic Epoxidation. In a typical catalytic run, the olefin (0.96 mmol), decane (0.17 mmol), and the precatalyst (9.6 μmol , 1 mol %) were dissolved in dry, freshly distilled CH_2Cl_2 (5 mL) under argon. Aqueous hydrogen peroxide (Perhydrol Merck, 30%, 9.8 M solution; 0.7 mL, 6.86 mmol) was added in one portion to the brown solution with vigorous stirring. In the alternative in situ procedure, **3a,b** were prepared from **2a,b** (19 μmol) and $\text{Ti}[\text{PF}_6]$ (6.6 mg, 19 μmol)

in CH_2Cl_2 (5 mL). The suspension was stirred overnight and filtered over Celite (to remove TiCl) into a CH_2Cl_2 solution (5 mL) of the olefin (1.9 mmol) and decane (0.34 mmol, internal standard). The aqua derivative **5c** was prepared in situ from the 6:3:1 mixture of **4**, *cis*- β -**2c**, and *trans*-**2c** described above (20 mg, ca. 20 μmol) and $\text{Ti}[\text{PF}_6]$ (7 mg, 20 μmol) by stirring overnight in CH_2Cl_2 (5 mL). The resulting solution was filtered (over Celite, to remove TiCl) into a CH_2Cl_2 solution (5 mL) of the olefin (1.92 mmol) and decane (0.34 mmol), and H_2O_2 (1.4 mL, 3.2 mmol) was added in one portion.

All reactions were monitored by GC for at least 6 h. Unreacted olefin and products (epoxide and aldehyde) were quantified by achiral GC (cross-linked silicon column) using decane as internal standard. The enantiomeric excess of the epoxide was determined by chiral GC (Alpha-Dex120 Supelco). Details are given in the Supporting Information.

Acknowledgment. S.B. and R.M.S. gratefully acknowledge financial support from the Swiss National Science Foundation.

Supporting Information Available: Details of the X-ray study of **4** and details of catalytic reactions and analytic procedures. This material is available free of charge via the Internet at <http://pubs.acs.org>.

OM000481V